Journal of Applied Mechanics and Technical Physics, Vol. 41, No. 4, 2000

DIFFRACTION OF SURFACE WAVES ON AN INHOMOGENEOUS ELASTIC PLATE

I. V. Sturova

UDC 532.59:539.3:534.1

The oblique incidence of small-amplitude waves on an elastic semi-infinite composite plate floating on the free surface of finite-depth water is studied. The front part of a constant-width plate is hinged to the basic part and has characteristics different from those of the basic part. The reflection and transmission coefficients of the waves and the vertical displacements of the plate are determined. It is shown that the heterogeneity of the plate material exerts a strong effect on surface-wave diffraction. Methods for decreasing the elastic deformations of the basic part of the plate are proposed.

The problem of surface-wave diffraction by a thin elastic plate located on the free surface of water is of interest for studying the behavior of an ice sheet and man-made structures such as floating platforms. In the linear approximation, this problem for a homogeneous plate in the form of a half-plane or band has been examined quite adequately [1, 2]. In the ice sheet, the heterogeneities appear as a result of cracking, breaking, and hummocking. The effect of these heterogeneities has been considered in [3–6]. For artificial structures, the heterogeneities of material can be more diverse and even created artificially with a view toward decreasing the elastic deformation in the middle part of a floating platform.

In this paper, the oblique incidence of monochromatic surface waves on a semi-infinite elastic plate whose front part is a freely supported band with characteristics different from those of the basic part is studied.

Formulation of the Problem. An elastic semi-infinite composite plate whose settling is assumed to be negligible floats on the free surface of a basin of constant depth H. A progressive wave with frequency ω is incident from the side of the free surface of the basin at an angle to the rectilinear edge of the plate. The coordinate system is chosen in such a way that the coordinate origin is located at the basin bottom under the plate edge, the x and y axes are perpendicular and parallel to it, respectively, and the z axis is directed vertically upward. The plate consists of two parts: the front part of constant width L is characterized by Young modulus E_1, thickness h_1, density ρ_1, Poisson's ratio ν_1; the other part of the plate has, respectively, the following characteristics: E_2, h_2, ρ_2, and ν_2. The edges of the plate components are freely supported on the line $x = L$, $z = H$.

The incoming wave propagates at an angle θ to the x axis and is determined by the velocity potential

$$\Phi_0(\boldsymbol{x}, t) = \varphi_0(x, z) \exp[i(\omega t - \beta y)].$$

Here

$$\varphi_0 = \frac{iag \cosh(k_0 z)}{\omega \cosh(k_0 H)} \exp(-i\alpha x), \quad (\alpha, \beta) = k_0(\cos\theta, \sin\theta), \quad \boldsymbol{x} = (x, y, z).$$

Lavrent'ev Institute of Hydrodynamics, Siberian Division, Russian Academy of Sciences, Novosibirsk 630090. Translated from Prikladnaya Mekhanika i Tekhnicheskaya Fizika, Vol. 41, No. 4, pp. 42–48, July–August, 2000. Original article submitted September 16, 1999.

[a is the wave amplitude, g is the acceleration of gravity, and the wavenumber k_0 is the positive root of the equation $\omega^2 = gk_0 \tanh(k_0 H)$]. Hereinafter, in the expressions that contain the factor $\exp(i\omega t)$, only the real part has a physical meaning.

We consider steady waves, and since the elastic-plate length is infinite, the velocity potential of the perturbed motion of the fluid is sought in the form

$$\Phi(\boldsymbol{x}, t) = \varphi(x, z) \exp[i(\omega t - \beta y)].$$

For determination of $\varphi(x, z)$, it is necessary to solve the equation

$$\frac{\partial^2 \varphi}{\partial x^2} + \frac{\partial^2 \varphi}{\partial z^2} - \beta^2 \varphi = 0$$

with the boundary conditions

$$\frac{\partial \varphi}{\partial z} - \frac{\omega^2}{g}\varphi = 0 \qquad (x < 0, \quad z = H),$$

$$\left[D_1\left(\frac{\partial^2}{\partial x^2} - \beta^2\right)^2 + 1 - \mu_1\omega^2\right]\frac{\partial \varphi}{\partial z} - \frac{\omega^2}{g}\varphi = 0 \qquad (0 < x < L, \quad z = H),$$

$$\left[D_2\left(\frac{\partial^2}{\partial x^2} - \beta^2\right)^2 + 1 - \mu_2\omega^2\right]\frac{\partial \varphi}{\partial z} - \frac{\omega^2}{g}\varphi = 0 \qquad (x > L, \quad z = H),$$

$$\frac{\partial \varphi}{\partial z} = 0 \qquad (z = 0),$$

where $D_j = E_j h_j^3/(12\rho g(1-\nu_j^2))$, $\mu_j = \rho_j h_j/(\rho g)$ $(j = 1, 2)$, and ρ is the water density. The plate is assumed to contact with water at any point and at any moments of time. The contact-boundary conditions, which are reduced to specifying the shear forces, bending moments, and vertical displacements, should be satisfied at the edges of separate parts of the plate.

Contact-Boundary Conditions. According to [4, 6], the following conditions for vertical displacements of the plate $\eta(x, y, t)$ are met on the hinged-joint line of the plate parts for $x = L$ and $z = H$:

$$\eta^+ = \eta^-; \tag{1}$$

$$D_1\left(\frac{\partial^2}{\partial x^2} + \nu_1 \frac{\partial^2}{\partial y^2}\right)\eta^- = D_2\left(\frac{\partial^2}{\partial x^2} + \nu_2 \frac{\partial^2}{\partial y^2}\right)\eta^+; \tag{2}$$

$$D_1 \frac{\partial}{\partial x}\left(\frac{\partial^2}{\partial x^2} + \nu_1' \frac{\partial^2}{\partial y^2}\right)\eta^- = D_2 \frac{\partial}{\partial x}\left(\frac{\partial^2}{\partial x^2} + \nu_2' \frac{\partial^2}{\partial y^2}\right)\eta^+; \tag{3}$$

$$D_2\left(\frac{\partial^2}{\partial x^2} + \nu_2 \frac{\partial^2}{\partial y^2}\right)\eta^+ = \chi\left(\frac{\partial \eta^+}{\partial x} - \frac{\partial \eta^-}{\partial x}\right). \tag{4}$$

Here $\eta^{\pm} = \lim\limits_{x \to L \pm 0} \eta$, χ is the rigidity coefficient of the hinged joint, and $\nu_j' = 2 - \nu_j$ $(j = 1, 2)$. Condition (1) means continuous vertical displacements of the plate parts on the line of contact, condition (2) implies equal bending moments at the edges of the contacting parts, condition (3) means the zero sum of the shear forces, and condition (4) assumes elastic hinging.

We now consider some particular cases. As $\chi \to \infty$, the plate parts are rigidly joined (for an ice sheet, this is the case of frozen-together ice floes [3]) and, according to condition (4), we have

$$\frac{\partial \eta^+}{\partial x} = \frac{\partial \eta^-}{\partial x}.$$

Conditions (1)–(3) preserve their form.

For $\chi = 0$, we have free hinging, which corresponds to the superposition of ice floes [5] in the case of an ice sheet, and conditions (2) and (4) take the form

$$D_1\left(\frac{\partial^2}{\partial x^2} + \nu_1 \frac{\partial^2}{\partial y^2}\right)\eta^- = D_2\left(\frac{\partial^2}{\partial x^2} + \nu_2 \frac{\partial^2}{\partial y^2}\right)\eta^+ = 0.$$

This is the free-edge condition which assumes the zero bending moment. The second free-edge condition, which assumes the zero shear force, should also be satisfied at the front edge of the plate:

$$\Big(\frac{\partial^2}{\partial x^2}+\nu_1\frac{\partial^2}{\partial y^2}\Big)\eta=\frac{\partial}{\partial x}\Big(\frac{\partial^2}{\partial x^2}+\nu_1'\frac{\partial^2}{\partial y^2}\Big)\eta=0\quad(x=0,\quad z=H).$$

The Method of Solution. To solve the posed problem, the conjunction method [2] is used. The region S, which is occupied by the fluid, is divided into three parts: S_1 $(-\infty<x<0)$, S_2 $(0<x<L)$, and S_3 $(L<x<\infty)$; in each region, $\varphi(x,z)$ is denoted by $\varphi_l(x,z)$ $(l=\overline{1.3})$.

Using the relation $\partial\eta/\partial t=\partial\Phi/\partial z|_{z=H}$, we express the contact-boundary conditions in terms of the values of the potentials at the edges of the corresponding parts of the plate for $z=H$:

$$\frac{\partial}{\partial z}\Big(\frac{\partial^2\varphi_2}{\partial x^2}-\nu_1\beta^2\varphi_2\Big)=\frac{\partial^2}{\partial x\,\partial z}\Big(\frac{\partial^2\varphi_2}{\partial x^2}-\nu_1'\beta^2\varphi_2\Big)=0\quad(x=0),$$

$$\frac{\partial\varphi_2}{\partial z}=\frac{\partial\varphi_3}{\partial z}\quad(x=L),$$

$$D_1\frac{\partial}{\partial z}\Big(\frac{\partial^2\varphi_2}{\partial x^2}-\nu_1\beta^2\varphi_2\Big)=D_2\frac{\partial}{\partial z}\Big(\frac{\partial^2\varphi_3}{\partial x^2}-\nu_2\beta^2\varphi_3\Big)\quad(x=L),$$

$$D_1\frac{\partial^2}{\partial x\partial z}\Big(\frac{\partial^2\varphi_2}{\partial x^2}-\nu_1'\beta^2\varphi_2\Big)=D_2\frac{\partial^2}{\partial x\,\partial z}\Big(\frac{\partial^2\varphi_3}{\partial x^2}-\nu_2'\beta^2\varphi_3\Big)\quad(x=L),$$

$$D_2\frac{\partial}{\partial z}\Big(\frac{\partial^2\varphi_3}{\partial x^2}-\nu_2\beta^2\varphi_3\Big)=\chi\frac{\partial^2}{\partial x\,\partial z}(\varphi_3-\varphi_2)\quad(x=L).$$

We now pass to dimensionless variables with the use of the basin depth H as a scale of length and $\sqrt{H/g}$ as a scale of time.

The functions φ_l are sought in the form of an expansion in terms of eigenfunctions of the corresponding boundary-value problems:

$$\varphi_1=[E_0\exp(-i\alpha x)+A_0\exp(i\alpha x)]Y_0(k_0,z)+\sum_{n=1}^{\infty}A_n\exp(\alpha_n x)Y_1(k_n,z),$$

$$\varphi_2=[B_0\exp(-iq_0^{(1)}x)+C_0\exp(iq_0^{(1)}x)]Y_0(r_0^{(1)},z)+\sum_{m=1}^{1}G_m\exp(s_m^{(1)}x)\cos(p_m^{(1)}z)$$
$$+\sum_{n=1}^{\infty}[B_n\exp(-q_n^{(1)}x)+C_n\exp(q_n^{(1)}x)]Y_1(r_n^{(1)},z),\tag{5}$$

$$\varphi_3=F_0\exp(-iq_0^{(2)}x)Y_0(r_0^{(2)},z)+\sum_{m=3}^{4}K_m\exp(s_m^{(2)}x)\cos(p_m^{(2)}z)+\sum_{n=1}^{\infty}F_n\exp(-q_n^{(2)}x)Y_1(r_n^{(2)},z).$$

Here $E_0=ia\sqrt{\Lambda_0(k_0)}/(\omega\cosh k_0)$, k_n $(n=1,2,\ldots)$ are the real roots of the equation $\omega^2=-k_n\tan k_n$ and $\alpha_n=\sqrt{k_n^2+\beta^2}$; $r_0^{(j)}$ $(j=1,2)$ are the positive roots of the equation

$$\omega^2=\frac{(1+\delta_j r^4)r\tanh r}{1+\gamma_j r\tanh r};\tag{6}$$

$$q_0^{(j)}=\sqrt{(r_0^{(j)})^2-\beta^2},\tag{7}$$

$\delta_j=D_j/H^4$, and $\gamma_j=\mu_j g/H$. Equation (6) also has an infinite number of purely imaginary roots $\pm ir_n^{(j)}$ $(n=1,2,\ldots)$ and $q_n^{(j)}=\sqrt{(r_n^{(j)})^2+\beta^2}$ and four complex roots $\pm\sigma^{(j)}\pm i\lambda^{(j)}$ $[\sigma^{(j)}>0,\ \lambda^{(j)}>0]$. The

quantities $p_m^{(j)} = \pm\lambda^{(j)} \mp i\sigma^{(j)}$ and $s_m^{(j)} = \sqrt{(p_m^{(j)})^2 + \beta^2}$. We number $s_m^{(j)}$ as follows: $s_{1,2}^{(j)} = c^{(j)} \pm id^{(j)}$, $s_{3,4}^{(j)} = -c^{(j)} \pm id^{(j)}$ [$c^{(j)} > 0$ and $d^{(j)} > 0$]. The functions Y_0 and Y_n ($n = 1, 2, \ldots$) have the form

$$Y_0(\xi, z) = \frac{\cosh(\xi z)}{\sqrt{\Lambda_0(\xi)}}, \qquad \Lambda_0(\xi) = \int_0^1 \cosh^2(\xi z)\, dz = \frac{1}{2} + \frac{\sinh(2\xi)}{4\xi},$$

$$Y_1(\xi, z) = \frac{\cos(\xi z)}{\sqrt{\Lambda_1(\xi)}}, \qquad \Lambda_1(\xi) = \int_0^1 \cos^2(\xi z)\, dz = \frac{1}{2} + \frac{\sin(2\xi)}{4\xi}.$$

The properties of eigenvalues and eigenfunctions have been studied in detail (see, e.g., [2]). The modes related to k_n and $r_n^{(j)}$ are called edge modes, and the modes defined by the complex roots $p_m^{(j)}$ are called growing or damping progressive waves, depending on the sign $\mathrm{Re}(s_m^{(j)})$. For the numbering introduced, the modes determined by $s_1^{(j)}$ and $s_2^{(j)}$ are growing modes, and those determined by $s_3^{(j)}$ and $s_4^{(j)}$ are damping modes. Relations (5) are written with allowance for the generation condition which implies the absence of an incoming wave from the region $x > L$, and the bounded potentials φ_1 as $x \to -\infty$ and φ_3 as $x \to \infty$. The modes related to $r_0^{(j)}$ are progressive flexural-gravitational waves at real values of $q_0^{(j)}$ in (7). For $r_0^{(j)} < \beta$, the values of $q_0^{(j)}$, however, become imaginary, which corresponds to the edge mode. The value of the angle $\theta = \theta_j$, where

$$\theta_j = \arcsin(r_0^{(j)}/k_0), \tag{8}$$

is called a critical value for the appropriate parts of the plate.

By virtue of the continuous motion of the fluid in the region S, the continuity conditions for the potentials and velocities of the horizontal wave flows are set at the boundaries of the regions S_l:

$$\varphi_1 = \varphi_2, \qquad \frac{\partial\varphi_1}{\partial x} = \frac{\partial\varphi_2}{\partial x} \qquad (x = 0, \quad 0 \leqslant z \leqslant 1); \tag{9}$$

$$\varphi_2 = \varphi_3, \qquad \frac{\partial\varphi_2}{\partial x} = \frac{\partial\varphi_3}{\partial x} \qquad (x = L, \quad 0 \leqslant z \leqslant 1). \tag{10}$$

Using the reduction method, we replace the infinite series in (5) by the finite sums with N terms. The coordination conditions (9) and (10) are satisfied in the integral meaning [they are multiplied sequentially by the functions $Y_0(k_0, z)$, $Y_0(r_0^{(j)}, z)$, $Y_1(k_n, z)$, and $Y_1(r_n^{(j)}, z)$ ($n = \overline{1, N}$) and integrated on the interval $0 \leqslant z \leqslant 1$]. As a result, the problem is reduced to a linear system of $4N + 10$ equations, which is solved numerically.

After all the desired complex coefficients in (5) are calculated, one can determine the wave motion of the fluid and the deformations of the plate. As is noted in [4], the contact-boundary conditions (1)–(4) are dissipation-free; therefore, the energy flux should be preserved upon passage over the plane $x = L$. Therefore, the energy relation [7]

$$|R|^2 + Q|T|^2 = 1, \tag{11}$$

which is inherent in a semi-infinite homogeneous plate, where the reflection coefficient of a surface wave R and the transmission coefficient of a flexural-gravitational wave T are, respectively, equal to

$$R = \frac{A_0}{E_0}, \qquad T = \frac{r_0^{(2)} F_0 \sinh r_0^{(2)}}{k_0 E_0 \sinh k_0} \sqrt{\frac{\Lambda_0(k_0)}{\Lambda_0(r_0^{(2)})}},$$

$$Q = \mathrm{Re}(q_0^{(2)}) k_0^2 \sinh(2k_0)\, \frac{2r_0^{(2)}(\delta_2 (r_0^{(2)})^4 + 1 - \gamma_2\omega^2) + \sinh(2r_0^{(2)})(5\delta_2 (r_0^{(2)})^4 + 1 - \gamma_2\omega^2)}{\mathrm{Re}(\alpha)(r_0^{(2)})^2 \sinh(2r_0^{(2)})[2k_0 + \sinh(2k_0)]},$$

should be satisfied.

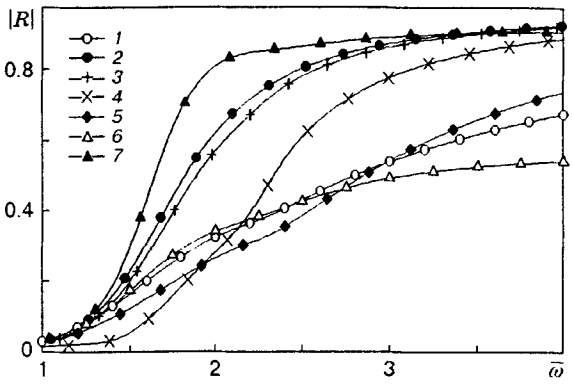

Fig. 1

The approximate method of determining the reflection and transmission coefficients is the solution of the problem considered without allowing for boundary waves, i.e., the infinite sums in representations (5). The solution of this problem is simpler, because it is reduced to a system of only 10 linear equations.

Numerical Calculations. In the calculations, the characteristics of the plate are the same as those in the experiment of [8] (hereinafter, we shall return to dimensional variables): $E_2 = 103$ MPa, $h_2 = 3.8$ cm, and $\rho_2 = 220$ kg/m^3. The thickness of the water layer in the channel was $H = 1.1$ m. For these values, we have $\delta_2 = 3.6 \cdot 10^{-2}$ and $\gamma_2 = 7.6 \cdot 10^{-3}$. The numerical and experimental values of the vertical displacements and bending moments upon normal incidence of surface waves on a homogeneous band 10 m wide are compared in [9].

We assume that the plate front part of width $L = 1$ m is hinged to the basic part; note that the Young modulus can be either equal or unequal to E_2. The other parameters of this part correspond to those of the basic plate: $h_1 = h_2$, $\rho_1 = \rho_2$, and $\nu_1 = \nu_2 = 0.3$.

Figure 1 shows the dependence of the reflection-coefficient modulus $|R|$ on $\bar{\omega} = \omega\sqrt{H/g}$ upon normal incidence of waves ($\theta = 0$) and $E_1 = E_2$. Curve 1 corresponds to rigid joining of the plates, curve 2 to free hinging, and curves 3–5 to elastic hinging with the dimensionless rigidity coefficients $\vartheta = \chi/H^3 = 10^{-3}$, 10^{-2}, and 10^{-1}. The approximate solutions without the edge modes are represented by curves 6 and 7 for rigid and free hinging, respectively. As is done in [2], these solutions can be applied only to fairly long waves.

The effect of oblique incidence ($\theta = 15°$) is shown in Fig. 2a–c for $E_1 = E_2$, $E_1/E_2 = 0.1$, and $E_1/E_2 = 10$, respectively. The notation of the curves 1–5 in Fig. 2 is the same as that in Fig. 1. The values of $|R|$ for $\bar{\omega} < 1$ are omitted in Figs. 1 and 2, because they do not exceed 0.1. According to (8), the critical angle $\theta_2 = 15°$ corresponds to $\bar{\omega}_1 \approx 3.413$, and $\theta_1 = 15°$ to $\bar{\omega}_2 \approx 4.560$ ($E_1/E_2 = 0.1$) and $\bar{\omega}_3 \approx 2.580$ ($E_1/E_2 = 10$). One can see that, changing the elasticity properties of the front part and the characteristics of the hinged joint, one can vary the reflection coefficient of the surface waves from the plate within a wide range and, hence, control the amount of energy transferred inside the basic part of the plate. The increase in the rigidity coefficient of the hinged joint allows a smooth passage from free hinging to rigid joining of the plate parts.

The vertical displacements of the plate can be presented in the form

$$\eta(x, y, t) = \mathrm{Re}\{\zeta(x) \exp[i(\omega t - \beta y)]\}.$$

The distribution of the amplitude of vertical displacements $|\zeta|/a$ on the site $0 \leqslant x/H \leqslant 2$ is shown in Fig. 3a and b, respectively, for normally and obliquely ($\theta = 15°$) incident surface waves with the period $\tau = 2\pi/\omega = 0.7$ sec for $\bar{\omega} \approx 3.006$. Curves 1–3 in Fig. 3 refer to calculation results for rigid joining of the plate parts for $E_1/E_2 = 0.1$, 1, and 10, and curves 4–6 refer to calculation results for free hinging at the same parameters. One can see that far from the leading edge, the amplitudes of the vertical displacements of the plate are affected by the composite character of the plate negligibly if the surface waves are reflected partially. For normally incident waves, a decrease in the amplitude of vertical displacements is observed only

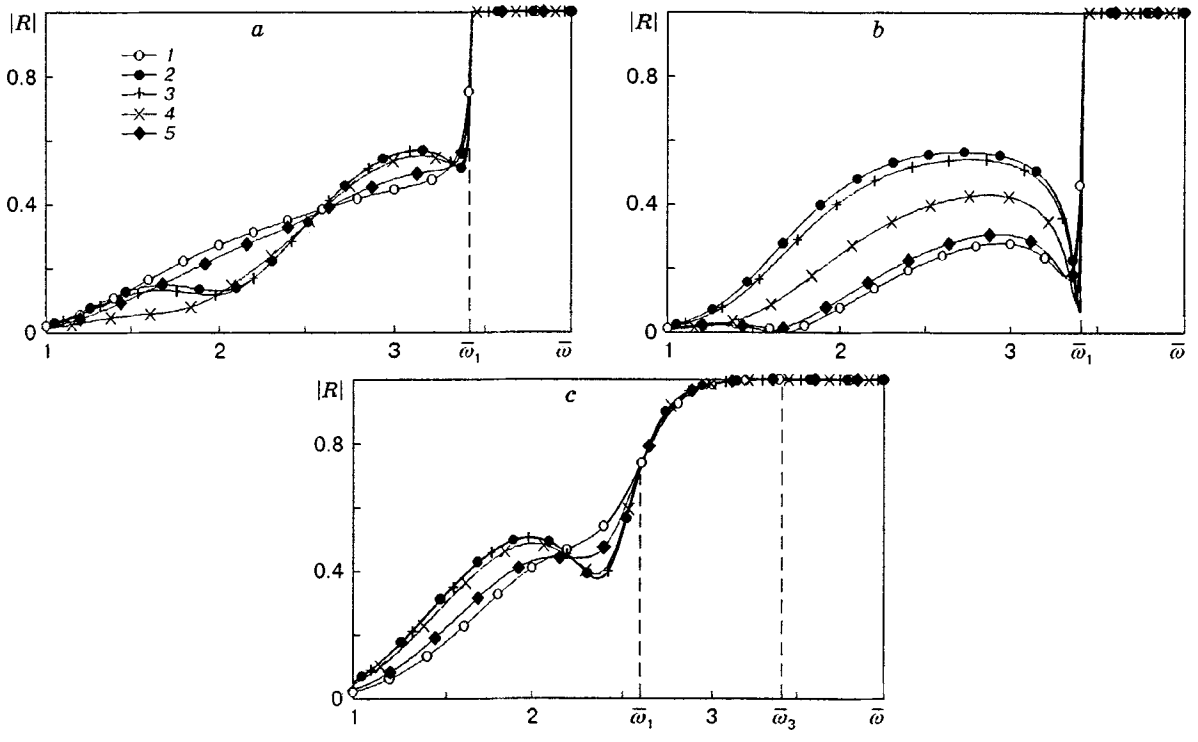

Fig. 2

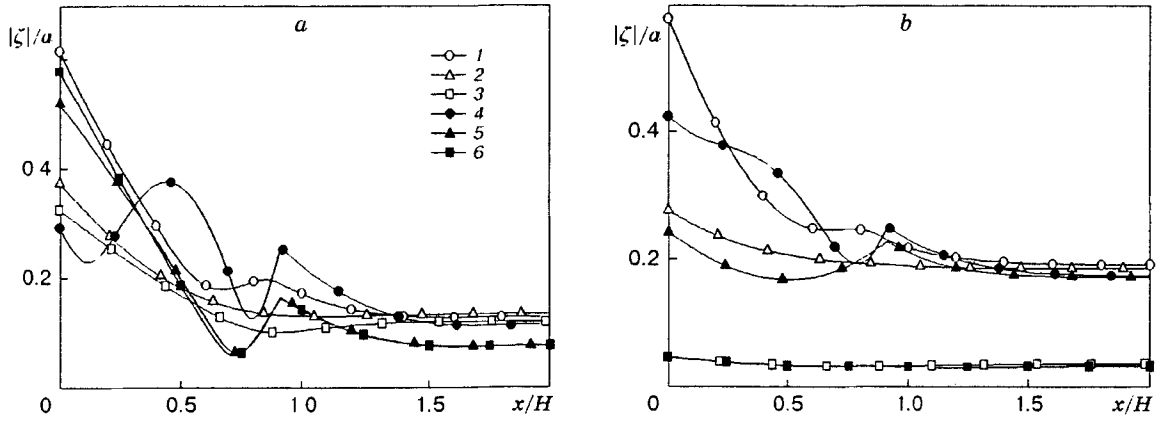

Fig. 3

for hinging (curves 5 and 6 in Fig. 3a; $|R| \approx 0.876$ and 0.882 for $E_1/E_2 = 1$ and 10, respectively). The most considerable decrease in plate oscillations occurs for obliquely incident waves and for a leading edge more rigid than the basic plate when the angle of incidence of the waves exceeds the critical value (curves 3 and 6 in Fig. 3b).

The calculation accuracy with allowance for the edge modes was checked by increasing their number in sequence; it was assumed to be $N = 30$ in this work, and the error of satisfaction of the energy relation (11) did not exceed 3%.

This work was supported by the Russian Foundation for Fundamental Research (Grant No. 97-01-00897) and Integration Project No. 43 of the Siberian Division of the Russian Academy of Sciences.

REFERENCES

1. V. A. Squire, J. P. Dugan, P. Wadhams, et al., "Of ocean waves and sea ice," *Annu. Rev. Fluid Mech.*, **27**, 115–168 (1995).
2. I. V. Sturov, "Oblique incidence of surface waves on an elastic plate," *Prikl. Mekh. Tekh. Fiz.*, **40**, No. 4, 62–68 (1999).
3. A. V. Marchenko, "Diffraction of surface waves on cracked ice," *Izv. Akad. Nauk SSSR, Mekh. Zhidk. Gaza*, No. 2, 93–102 (1993).
4. A. V. Marchenko, "Diffraction of flexural-gravitational waves on linear heterogeneities in ice," *Izv. Ross. Akad. Na[illegible]kh. Zhidk. Gaza*, No. 4, 97–112 (1997).
5. A. E. Bukatov and D. D. Zav'yalov, "Incidence of flexural-gravitational waves on the line of contact of two floating ice plates of different thickness, *Morskoi Gidrofiz. Zh.*, No. 1, 11–17 (1998).
6. A. Marchenko, *Flexural-Gravitational Waves. Wave Dynamics on a Liquid Surface* [in Russian], Nauka, Moscow (1999), pp. 65–111.
7. C. Fox and V. A. Squire, "On oblique reflexion and transmission of ocean waves at shore fast sea ice," *Philos. Trans. Roy. Soc. London, Ser. A*, **347**, No. 1682, 185–218 (1994).
8. C. Wu, E. Watanabe, and T. Utsunomiya, "An eigenfunction expansion-matching method for analyzing the wave-induced responses of an elastic floating plate," *Appl. Ocean Res.*, **17**, No. 5, 301–310 (1995).
9. I. V. Sturova, "The oblique incidence of surface waves onto the elastic band," in: *Proc. of the 2nd Int. Conf. on Hydroelasticity in Marine Technology* (Fukuoka, Japan, 1–3 Dec., 1998). Res. Inst. Appl. Mech., Kyushu Univ., Fukuoka (1998), pp. 239–245.